"Integrative Genomic Analysis for the Bioprospection of Regulators and Accessory Enzymes Associated with Cellulose Degradation in a Filamentous Fungus (*Trichoderma harzianum*)"

Jaire A. Ferreira Filho[1,2], Maria Augusta C. Horta[1,3], Clelton A. dos Santos[1], Deborah A. Almeida[1,2], Natália F. Murad[1], Juliano S. Mendes[1], Danilo A. Sforça[1], Claudio Benício C. Silva[1], Aline Crucello[1], Anete P. de Souza[1,4,*]

[1]Center for Molecular Biology and Genetic Engineering (CBMEG), University of Campinas (UNICAMP), Campinas, SP, Brazil

[2]Graduate Program in Genetics and Molecular Biology, Institute of Biology, UNICAMP, Campinas, SP, Brazil

[3]Holzforshung München, TUM School of Life Sciences Weihenstephan, Technische Universität München, 85354 Freising, Germany

[4]Department of Plant Biology, Institute of Biology, UNICAMP, Campinas, SP, Brazil

*** Correspondence:**

Profa Anete Pereira de Souza

Dept. de Biologia Vegetal

Universidade Estadual de Campinas

CEP 13083-875

Campinas, São Paulo, Brazil

Tel.: +55-19-3521-1132

E-mail:anete@unicamp.br

Abstract

Background: Unveiling fungal genome structure and function reveals the potential biotechnological use of fungi. *Trichoderma harzianum* is a powerful CAZyme-producing fungus. We studied the genomic regions in *T. harzianum* IOC3844 containing CAZyme genes, transcription factors and transporters.

Results: We used bioinformatics tools to mine the *T. harzianum* genome for potential genomics, transcriptomics, and exoproteomics data and coexpression networks. The DNA was sequenced by PacBio SMRT technology for multi-omics data analysis and integration. In total, 1676 genes were annotated in the genomic regions analyzed; 222 were identified as CAZymes in *T. harzianum* IOC3844. When comparing transcriptome data under cellulose or glucose conditions, 114 genes were differentially expressed in cellulose, with 51 CAZymes. CLR2, a transcription factor physically and phylogenetically conserved in *T. harzianum* spp., was differentially expressed under cellulose conditions. The genes induced/repressed under cellulose conditions included those important for plant biomass degradation, including CIP2 of the CE15 family and a copper-dependent LPMO of the AA9 family.

Conclusions: Our results provide new insights into the relationship between genomic organization and hydrolytic enzyme expression and regulation in *T. harzianum* IOC3844. Our results can improve plant biomass degradation, which is fundamental for developing more efficient strains and/or enzymatic cocktails for the production of hydrolytic enzymes.

Keywords: cellulose degradation, CAZymes, genomic, transcriptome, fungi

Background

Trichoderma harzianum is a common fungal species in soil and is used as a biological control in a variety of phytopathogenic fungi [1]. However, the use of lignocellulosic biomass degradation is still poorly explored when compared to that of other cellulolytic fungi. Due to the high cellulolytic activity of some strains, *T. harzianum* has shown considerable potential for application in plant biomass hydrolysis [2-4]. *T. harzianum* strains have potential for the production of an enzymatic/protein arsenal necessary for the complete hydrolysis of cellulosic compounds in fermentable sugars [5-10].

Currently, the most-studied and widely used industrial-scale enzymes are produced by the fungus *T. reesei* and species from the *Aspergillus* genus. These organisms are the source of the majority of enzymes that make up enzymatic cocktails that are available on the market [11]. *T. reesei* is a widely studied fungus and is found in several works in genomics, transcriptomics, proteomics and metabolic engineering [12-16]. Thus, increasing the number of biotechnological studies related to this bioprocess for *T. harzianum* is necessary.

The three main groups involved in the hydrolysis of cellulose (CEL) are cellobiohydrolases, endo-β-1,4-glucanases and β-glucosidases. In addition, accessory enzymes such as copper-dependent lytic polysaccharide mono-oxygenases (LPMOs), cellulose-induced protein 1 and 2 (CIP1 and CIP2) and swollenin also participate in this process [17-20].

One of the great challenges in understanding the molecular mechanism of biomass degradation is how the transcription factors (TFs) related to this system act. Several fungal TFs have been identified as related to the degradation of plant biomass, many of which belong to the binuclear zinc family [21]. Many TFs have been described as being directly involved in the regulation of plant biomass [22]. This number has been expanding rapidly in recent years, mainly due to the increase in the sequencing scale of whole genomes and the

exponential increase in bioinformatics tools for analysis, which produce massive amounts of information, and in the number of genes identified [22, 23].

The purpose of the present study was to analyze genomic regions with CAZyme genes using a bacterial artificial chromosome (BAC) library that we built [24] and to integrate these data with RNA-seq, secretome data and coregulation networks. We sequenced a massive amount of DNA and used it to integrate genomic data (genomic regions containing CAZymes), expression patterns (the transcriptome under degradation conditions), proteins (the secretome by mass spectrometry) and systems biology (with gene regulatory networks) to obtain a broad and precise overview of the CEL degradation pathways. Based on our study, we characterized the main genes, accessory enzymes and regions involved in the degradation and regulation process of hydrolytic enzymes. In addition, we analyzed the regulator cellulose degradation regulator 2 (CLR2) found in a cluster with other important enzymes. These results will be important for further studies of regulation and gene silencing.

Results

Genomic regions of T. harzianum IOC3844

In this study, a library of large genomic regions was used as a resource to search for genes of interest and to thoroughly study the genomic structure of *T. harzianum* IOC3844 (ThIOC3844) (accession numbers MK861589-MK861650 - Supplementary Table S1 and Fig. S1). Screening for genes of interest resulted in a total of 62 regions that contained CAZymes genes related to the degradation of plant biomass in the ThIOC3844 genome. Sequencing of these regions generated a total of 5 Mb of the estimated 40 Mb genome (Supplementary Table S2 and S3). These regions ranged in size from 43 to 152 kb, enabling

the prediction and annotation of 1676 gene models for this strain (Supplementary Table S4). The average number of genes per region was 26 (Supplementary Table S1).

The genome of *T. reesei* QM6a (PRJNA325840) was used to analyze the distribution of genes in ThIOC3844. This genome, which is composed of seven chromosomes with a total size of 34 Mb, was divided into 38 intervals (1 Mb) (Fig. 1). It was possible to observe CAZyme genes annotated in ThIOC3844 distributed throughout the whole genome. Only four intervals had no CAZyme genes, and when all the genes in the genomic regions of ThIOC3844 were mapped, genes were found in all intervals.

The genes were functionally annotated for the main gene ontologies: biological processes, cellular components and molecular functions (Fig. 2a and Supplementary Fig. S2). We found 209 sequences of hydrolytic activity, 139 related to transport proteins and 85 sequences involved in regulation of gene expression (possible TFs). In addition, a specific annotation was made for genes identified as enzymes, where hydrolases (40%), oxidoreductases (25%), transferases (22%), lyases (6%), ligases (4%) and isomerases (3%) (Figure 2b) were found. We also identified genes directly related to the degradation of CEL and hemicellulose, with action of α-L-arabinofuranosidase (EC 3.2.1.55), endo-1,4-β-xylanases (EC 3.2.1.8), cellobiohydrolases (3.2.1.91), endo-β-1,4-glucanase (EC 3.2.1.4) and β-glucosidase (EC 3.2.1.21) (Fig. 2c and Supplementary Table S5).

A total of 1676 genes were predicted. Of these, 222 were annotated as CAZymes in ThIOC3844, including 45% of GHs, 23% of GTs, 10% of CEs, 8% of AAs and 14% of CBMs (Fig. 3 and Supplementary Table S6). The GH class presented with the highest number of families, including GH2 (3 genes), GH7 (1 gene), GH3 (9 genes), GH5 (6 genes), GH12 (1 gene), GH18 (4 genes) and GH62 (1 gene).

Genomic comparison

For this analysis, we compared the genomic regions of ThIOC3844 against the entire genome of different strains and species of the genus *Trichoderma*. Genomic comparison of the sequenced regions of ThIOC3844 with two other strains of the same species (*T. harzianum* B97 – ThB97 and *T. harzianum* – T6766) showed a higher similarity to ThB97 (99.25%) than ThT6766 (91.61%). For the *T. atroviride* IMI206040 genome (TaIMI206040), the similarity to ThIOC3844 was 85.09%. For *T. virens* Gv29-8 (TvGv29-8), the similarity was 86.55%, and for *T. reesei* QM6a (TrQM6a), the similarity was 85.11%.

When we compared syntenic genes between groups of genes, a greater difference between *T. harzianum* and *T. atroviride* and *T. reesei* was observed. The *T. harzianum* TR274 (ThTR274) strain presented the same gene profile of genomic organization as that found in ThIOC3844. In TaIMI206040, four genes (GH4, transporter and two GH26) from the cluster were not found; for TvGv29-8, two genes were not found (GH1 and GH4). For *T. reesei* QM6a, three genes (GH4 and two GH26) were not found; in addition, the translocation of genes (MFS x GH2 and TF2 x CLR2) was found. The genes for the transcription factor CLR2, putative transcription factor TF2 and MFS (major facilitator superfamily permease) were maintained in all species analyzed. This result suggests a potential association between the regulation and expression of these genes (Fig. 4).

Expression by RNA-Seq and secreted proteins

All genes predicted in the genomic regions were analyzed according to expression data by RNA-Seq (under CEL and GLU degradation conditions) (Supplementary Table S7) and secreted proteins identified by mass spectrometry (LC-MS/MS). We found 114 genes with differential expression under CEL degradation conditions when compared to GLU degradation conditions; among them, 51 were classified as CAZymes, such as beta-glucosidase of the GH1 family (1.8-fold change - FC), LPMOs of the AA9 family (FC 5.0)

and hypothetical protein with domain CBM1 (FC 3.7). In addition, two differentially expressed TFs were identified, CLR2 (FC 1.6) and unidentified transcriptional regulator of zing finger – Zn2Cys6 (FC 2.3). Six transport proteins were also found (iron permease, MFS hexose transporter, siderophore transporter, ammonium permease, sugar transporter and siderophore iron transporter).

Among the genes annotated as CAZymes in ThIOC3844, 31 were found in the secretome of ThIOC3844 under CEL conditions, and the main families were GH3, GH12, CBM1, AA9, GH6/CBM1, GH45/CBM1, GH62 and GH5. In this analysis, we also used the level of expression of the secreted genes. The gene with the highest TPM index (1567.4 TPM) is a cellobiohydrolase (EC 3.2.1.91) of the GH6 family. However, our results indicate that genes with low expression levels are also important secreted enzymes (Table 1).

CLR2 transcription factor

The phylogenic analysis of the CLR2 factor showed a clear separation of this TF in relation to Basidiomycetes and Ascomycetes (Fig. 5a and Supplementary Table S8). However, even within these groups, considerable phylogenetic diversity was observed among the species of analyzed fungi with a variety of clades within the same group. Different strains of *T. harzianum* grouped in a single clade with proximity to *T. reesei* and *T. atroviride* species. Our results show a wide range of functional variety for CLR2, which may indicate different types of performance between species.

A structural modeling analysis for the CLR2 protein of ThIOC3844 was performed using *T. reesei* as a comparator. For both proteins, the best template was 6F07 (*Saccharomyces cerevisiae*), with e-values of $4.07e^{-06}$ and $6.62e^{-06}$ for ThIOC3844 (Figure 5b) and *T. reesei* (Figure 5c), respectively. Prediction of 1 and 3 protein domains was made for ThIOC3844 and *T. reesei*, respectively. For ThIOC3844, 59% of the residues were

already modeled, and for *T. reesei*, it was possible to model 83%. For ThIOC3844, the secondary structure prediction was 46% H (helix), 0% E (beta-sheet) and 53% C (loop), and for solvent access, it was 56% E (exposed), 19% M (medium) and 23% B (buried).

A coregulation network of genes directly related to the CLR2 regulator was constructed, searching for insights about other important proteins in the process of cellulase expression. We identified 36 genes directly linked to CLR2, of which 21 genes were annotated as hypothetical proteins. In addition, we found that genes with known annotations were related to the process of gene expression, including genes annotated as initiation factors, kinases and helicases (Fig. 6a and Supplementary Table S9).

Network of induced/repressed genes in cellulose

Using the gene expression data of the secreted proteins, a Bayesian network of induced/repressed genes was constructed based on the CEL growth conditions for *T. harzianum* IOC3844 (Fig. 6b). The major genes that were induced under this condition belong to the GH7 (exoglucanase), GH5 (endo-β-1,4-glucanase), GH3 (β-glucosidase), GH12 (murein transglycosylase), CE15 (CIP2), AA9 (LPMO) and AA8 (hypothetical protein) families. In addition, seven genes that were not classified as CAZymes were also induced under CEL conditions. The families of repressed genes were GH10 (glycoside hydrolase 10 family endo-1,4-β-xylanase), GH11 (glycoside hydrolase 11 family endo-1,4-β-xylanase), GH76 (alcohol dehydrogenase 1), GH20 (β-N-acetylhexosaminidase) and GH35 (glycoside hydrolase 35).

Discussion

In the present study, an integrative multi-omics approach was used to mine CAZyme-rich regions of ThIOC3884. BAC clones were selected, sequenced and used in comparative

analyses focusing on the expression profile via RNA-Seq and the exoproteome under different fungal growth conditions, enabling the discovery of important gene/proteins related to plant biomass degradation (Supplementary Fig. S3).

The vast majority of important enzymes for the degradation of plant biomass are already known [25-27]. The current challenge is how enzymes are regulated and the genetic mechanism of their activation. Thus, many works with cellulolytic fungi have focused on TFs, accessory enzymes, transporters and the way the type of biomass affects the process of regulating the cellulases and hemicellulases [22, 28-30]. Other studies have already shown the potential of *T. harzianum* for the degradation of plant biomass. This is the first work that integrates results from different biotechnology approaches and that focuses on the prediction of the most important enzymes and TFs used by *T. harzianum* IOC3844 to degrade CEL.

The molecular process of CEL degradation is extremely complex and involves hydrolytic enzymes acting on the extracellular medium, carrier proteins and TFs (Figure 7). For *T. harzianum* and *T. reesei*, the major CAZy families related to CEL degradation were identified in the genome (GH1, GH3, GH6, GH7, GH12, GH45 and AA9) [7], and many of the cellulases have already had their three-dimensional structure solved; however, many key proteins in this process are not well known as transporter TFs related to the regulation of these enzymes.

The study of genomic regions is an important tool for providing a global view of the important genes and regulatory regions of a genome [24, 31]. The genomes of a few strains of *T. harzianum* are available [32, 33]. A complete genome draft sequenced in 1572 scaffolds is available for *T. harzianum* T6776 [32]; however, little is known about the ThIOC3844 genome, and as it is a strain with potential for hydrolytic enzymes, more genomic information regarding CAZyme sequences is needed. In this study, our strategy was to use large genomic regions and integrate these data with other genetic information.

A large number of fungal genomes have already been used as a platform to search for new genes related to the degradation of biomass, as is the case for *T. reesei* QM6a, which has a finalized genome divided into seven chromosomes [34]. Our study results with the genomic regions of ThIOC3844 showed a large number of enzymes classified as CAZymes, as well as TFs and transporters in clusters in the genome, which may be important for future studies of genetic modification of this lineage.

Analyzing the level of expression of certain genes under certain conditions is an important step in understanding how transcription is affected in a specific biological condition [17, 35]; however, there is not always a direct relationship between what is being highly expressed and the proteins that are important in the extracellular medium. Thus, in this work, in addition to studying the most expressed genes that we found in the genomic regions, we also searched for those with a confirmed presence in the fungus secretome CEL degradation conditions. Our results showed that CAZy families are key in the degradation of CEL, with a high level of expression and a positive presence as a secreted protein.

Genomic comparison is a powerful tool for understanding differences and evolutionary dynamics among related species [36-38]. Our data show a high similarity between different strains of *T. harzianum* (IOC3844, B97 and T6776), which indicates that differences in enzyme production and efficiency may be related more to gene regulation mechanisms than differences in the sequence itself. In addition, by synteny analysis, it was possible to observe a greater difference in relation to the genome of *T. reesei*, which can be explained by the loss of genes and genomic modifications carried out in lineages of this fungus to increase its productivities of enzymes related to plant biomass degradation [12, 39].

The CLR2 transcription factor was described as an important regulator in the expression of cellulases by *Neurospora crassa* [22]; however, its functional role is not yet clear for fungi of the genus *Trichoderma*, including *T. reesei* [14, 40]. In the genome of

ThIOC3844, we found a cluster with the CLR2 TF in association with other putative transcription factors, CAZymes, transporters and MFS permease. The same behavior was found for the *T. reesei* CLR2 TF, which has physical proximity and coexpression with a sugar transporter [29, 41]. These results indicate that there may be a mechanism for the joint regulation and expression of this TF with transporters related to biomass degradation. Based on RNA-Seq data, we observed differential expression of CLR2 in the cellulose condition. In this way, we analyzed the coregulation network of the CLR2 regulator. The present study illuminates unclear areas of the genomic organization, expression and putative regulation of CLR2 in *T. harzianum.*

Coregulation networks provide insights into how genes correlate and interact with each other [35, 42, 43]. We identified 36 genes directly associated with the CLR2 regulatory factor; these genes may be important in the regulation process of this factor, which is linked to the expression of cellulases in other filamentous fungi. Techniques such as gene knockout can further validate the functional or synergistic importance of these genes with key TFs for the expression of genes related to degradation of plant biomass.

Conclusions

Our results present an innovative approach in using different types of omics data to search for new important genes and genetic regulation mechanisms during the process of CEL degradation. We found several TFs, accessory enzymes and transporters in the genomic regions of ThIOC3844 that may be important for the expression/secretion of CAZyme genes. Among these, CLR2, CIP2 and LPMOs are promising candidates for further study. Our results indicate that the CRL2 regulator matches all the requirements for involvement in cellulose degradation by *T. harzianum*. In addition, through the approach of coregulation networks, it is possible to understand the relationship between genes and to find new targets

for biochemical characterization. The results allowed the identification of important genetic regions, key genes and functional proteins, and this information can be used for the development and improvement of enzymatic hydrolysis technology for the bioethanol industry.

Methods

T. harzianum strain and genomic resources

T. harzianum IOC3844 (ThIOC3844) was obtained from the Brazilian Collection of Environment and Industrial Microorganisms (CBMAI). A library of BACs consisting of 5,760 clones previously constructed for this fungus strain [24] was used to search for genomic regions. The genomic sequences of *T. harzianum* T6776 (PRJNA252551), *T. reesei* QM6a (PRJNA325840), *T. atroviride* IMI206040 (PRJNA19867) and *T. virens* Gv29-8 (PRJNA19983) were used for comparison with ThIOC3844.

BAC library screening for gene selection in T. harzianum IOC3844

We designed primers for 62 target CAZyme genes (Supplementary Table S1) using transcriptome data [3] to search for positive BAC clones that contain genes previously selected from the plate (with the complete BAC library comprising fifteen 384 plaques) and column pools (24 columns of each plate). The plate and column pools were amplified using the Illustra GenomiPhi HY DNA Amplification Kit (GE Healthcare Life Sciences, UK) following the manufacturer's instructions. The screening reactions for the search for positive clones were performed via PCR using the CFX384 Touch Real-Time PCR Detection System (Bio-Rad).

Single-molecule real-time (SMRT) sequencing and assembly

Libraries for sequencing were prepared according to the Pacific Biosciences (PacBio) protocol, and sequencing was performed at the Arizona Genomics Institute (AGI; Tucson, USA) using a Single-Molecule Real-Time (SMRT) DNA sequencing system available from PacBio. *De novo* assembly was performed with the PacBio Corrected Reads (PBcR) pipeline implemented as part of Wgs-assembler v8.3rc2 [44] and Celera Assembler [45]. The contigs obtained with the assemblers were subjected to error correction with pbalign (v0.2). The PacBio reads were aligned using the BLASR algorithm [46], and assembly polishing was performed with the Quiver tool (Supplementary Table S2 and S3) [47].

Gene prediction and functional annotation

The FGENESH tool was used for initial gene prediction analysis [48], followed by manual correction with the *T. harzianum* T6776 and *T. reesei* QM6a gene models. Annotations of the ontologies were performed with Blast2GO [49]. InterPro protein domains were predicted using InterProScan (http://www.ebi.ac.uk/interpro/) [50]. Information derived from the CAZy database was downloaded for each CAZyme family (www.cazy.org). The protein sequences of *T. harzianum* IOC3844 were used as queries in basic local alignment search tool (BLASTp) searches against the locally built CAZyme BLAST database. Only BLAST matches showing an e-value less than 10^{-11}, identity greater than 30% and queries covering greater than 70% of the sequence length were retained and classified according to the CAZyme catalytic group as glycoside hydrolases (GHs), glycosyl transferases (GTs), polysaccharide lyases (PLs), carbohydrate esterases (CEs), carbohydrate-binding modules (CBMs) or auxiliary activities (AAs).

***Genomic comparison in* Trichoderma spp.**

325 The software used for alignment was Nucmer (-maxmatch), which is part of the software
326 package MUMmmer 3.23 [51]. The delta-filter (-q), show-coords (-rcl), and DNADIFF
327 (standard parameters) were used for filtering, obtaining the mapping coordinates and
328 generating the statistical report in the alignment, respectively. SimpleSynteny software
329 (https://www.dveltri.com/simplesynteny/) [52] was used to compare a cluster of 12 genes
330 among different species of *Trichoderma* spp.
331
332 ***Phylogenetic analysis and structure modeling of CLR2***
333 The CLR2 sequences of ThIOC3844, *T. reesei* QM6a, *T. atroviride*, *T. virens* and other
334 species of fungi were used as the basis for constructing the phylogenetic trees. These fungi
335 were divided into Ascomycetes and Basidiomycetes. The sequences were aligned using
336 ClustalW [53] and analyzed with Molecular Evolutionary Genetics Analysis (MEGA)
337 software v7.0 (https://www.megasoftware.net/) [54]. The phylogenetic analyses were
338 performed in MEGA7 using the maximum likelihood (ML) [55] method of inference based
339 on the Jones-Taylor-Thornton (JTT) matrix-based model and 1000 bootstrap replicates [56]
340 for each analysis. Pairwise deletion was employed to address alignment gaps and missing
341 data. The trees were visualized and edited using the FigTree program
342 (http://tree.bio.ed.ac.uk/software/figtree/). *In silico* modeling of the domain of CLR2 was
343 performed using RaptorX protein structure prediction software (http://raptorx.uchicago.edu/)
344 [57].
345
346 ***RNA-Seq and exoproteome analysis***
347 The expression levels of ThIOC3844 were analyzed using RNA-Seq data (PRJNA336221)
348 obtained from a previous study in which the transcripts were obtained following growth of
349 the fungus on two different carbon sources, CEL and GLU [35]. The reads from the RNA-

Seq library were mapped against the ThIOC3844 genes using the CLC Genomics Workbench (https://www.qiagenbioinformatics.com/products/clc-genomics-workbench/) [58]. The expression values were expressed in reads per kilobase of exon model per million mapped reads (RPKM), and the normalized value for each sample was calculated in transcripts per million (TPM). For the analysis of differential expression, the following parameters were used: fold change greater than or equal to 1.5 and p-value lower than 0.05. The analysis of the exoproteome was performed by means of a BLASTn search of the predicted gene of ThIOC3844 against the local database of protein sequences from *T. harzianum* found in the extract of fungal growth under CEL and GLU conditions.

Gene regulatory network

The gene regulatory networks were assembled from the reference mapped RNA-Seq data using each set of biological triplicates for the CEL and GLU conditions [35]. The interaction between the genes was obtained by calculating Pearson's correlation for each pair of genes. The induction and repression networks were constructed based on the expression data of a set of genes that were identified in the secretome of the CEL growth condition by the Bayesian inference method [59]. If the secreted protein was present in the condition, it was assigned a value of one. If the secreted protein was absent, it was assigned a value of zero. The treatment conditions were considered as regulators of the network to detect the direct relationships between the conditions and the genes. Thus, the Bayesian network represents the relationships among the conditions, gene expression, and secreted proteins. Cytoscape software v 3.4.042 [60] (https://cytoscape.org/) was used for data analysis and construction of the CLR2 subnetwork.

375 **Additional files**

376 **Additional file 1: Fig S1.** Screening genes of interest in the genomic library of *T. harzianum*
377 IOC3844 by qPCR (a); reads size sequenced using PACBio technology (b); genes cluster in a
378 genomic region of *T. harzianum* (c). **Fig. S2.** Distribution of the main GO terms of the
379 annotated genes in *T. harzianum* IOC3844. **Fig. S3.** Pipeline approach for the analyzes used
380 in this work of genes and genomic study in *T. harzianum*. **Supplementary Table S2.**
381 Assembly parameters of a set of sequenced genomic region using PACBio technology.
382 **Supplementary Table S3.** Comparison of genomic data among different species of
383 *Trichoderma* spp. **Supplementary Table S8.** Description of the species used for the
384 phylogenetic analysis of the transcription factor CLR2. **Supplementary Table S9.**
385 Description of the genes found in the coregulation networks.

386 **Additional file 2: Supplementary Table S1.** Description of the genomic regions sequenced
387 in *T. harzianum* IOC3844.

388 **Additional file 3: Supplementary Table S4.** Annotation of all genes predicted in *T.*
389 *harzianum* IOC3844.

390 **Additional file 4: Supplementary Table S5.** Description of the EC codes for *T. harzianum*
391 IOC3844 genes.

392 **Additional file 5: Supplementary Table S6.** Description of the CAZymes genes for *T.*
393 *harzianum* IOC3844.

394 **Additional file 6: Supplementary Table S7.** Level of expression of the genes annotated in
395 *T. harzianum* IOC3844 by means of RNA-seq.

396

397 **List of abbreviations**

398 **AA:** Auxiliary enzymes; **B:** buried; **BAC:** bacterial artificial chromosome; **BLAST:** Basic
399 local alignment search tool; **bp:** Base pair; **BRENDA:** Braunschweig Enzyme Database; **C:**

loop; **CAZymes:** Carbohydrate-active enzymes; **CBMAI:** Brazilian Collection of Environment and Industrial Microorganisms; **CBM:** Carbohydrate-binding module; **CE:** Carbohydrate esterases; **CEL:** Cellulose; **CIP1:** cellulose-induced protein 1; **CIP2:** cellulose-induced protein 2; **CLR2:** cellulose degradation regulator 2; **DNA:** Deoxyribonucleic acid; **E:** beta-sheet; **EC:** Enzyme commission number; **Ex:** exposed; **FC:** fold change; **GH:** Glycoside hydrolases; **GLU:** Glucose; **GO:** gene ontologies; **GT:** Glycosyltransferases; **H:** helix; **JTT:** Jones-Taylor-Thornton; **kb:** Kilobases; **LPMO:** Lytic polysaccharides monooxygenase; **M:** medium; **Mb:** Megabase; **MEGA:** Molecular evolutionary genetics analysis; **MFS:** major facilitator superfamily permease; **ML:** maximum likelihood; **PacBio:** Pacific Biosciences; **PBcR:** PacBio Corrected Reads; **PCR:** Polymerase chain reaction; **PL:** Polysaccharide lyases; **RNA:** Ribonucleic acid; **RNA-Seq:** RNA sequencing; **RPKM:** Reads per kilobase of exon model per million mapped reads; **SMRT:** Single-Molecule Real-Time; **TaIMI206040:** *T. atroviride* IMI206040; **TFs:** transcription factors; **ThB97:** *T. harzianum* B97; **ThIOC3844:** *Trichoderma harzianum* IOC-3844; **ThTR274:** *T. harzianum* TR274; **Th6766:** *T. harzianum*; **TPM:** Transcripts per million; **TrQM6a:** *T. reesei* QM6a; **TvGv29-8:** *T. virens* Gv29-8

Declarations

Ethics approval and consent to participate

Not applicable

Consent for publication

Not applicable

425 ***Availability of data and materials***

426 The RNA-seq data can be accessed by the accession number PRJNA336221. Data from the
427 genomic regions were submitted to GenBank (https://www.ncbi.nlm.nih.gov/genbank/) under
428 the accession numbers MK861589-MK861650 (Supplementary Table S1).

429

430 ***Competing interests***

431 The authors declare that the research was conducted in the absence of any commercial or
432 financial relationships that could be construed as a potential conflict of interest.

433

434 ***Funding***

435 This work was supported by grants from the Fundação de Amparo à Pesquisa do Estado de
436 São Paulo (FAPESP 2015/09202-0), Coordenação de Aperfeiçoamento de Pessoal de Nível
437 Superior (CAPES) Computational Biology Program (CBP) and Conselho Nacional de
438 Desenvolvimento Científico e Tecnológico (CNPq). JAFF received a PhD fellowship from
439 CNPq (170565/2017-3) and a PD fellowship from CAPES (CBP - 88887.334235/2019-00);
440 MACH received a PD fellowship from CAPES (CBP) and a SWE PD fellowship from
441 CAPES, Computational Biology Program; CAS received a PD fellowship from FAPESP
442 (2016/19775-0) and a SWE PD fellowship from CAPES (CBP); DAA received partial MS
443 fellowship from FAPESP (17/17782-2) and partial MS fellowship from CAPES (CBP); NFM
444 received a PD fellowship from CNPq and CAPES (CBP); JSM received a PD fellowship
445 from CNPq and CAPES (CBP); CBCS received a PD fellowship from FAPESP (17/26781-0)
446 and CAPES (CBP); and APS is the recipient of a research fellowship from CNPq.

447

448 ***Authors' contributions***

449 APS and JAFF designed the study. JAFF, MACH, CAS, DAA, JSM, DAS and AC
450 performed the research. JAFF, MACH, CAS, DAA, NFM and CBCS analyzed the data.
451 JAFF, MACH, CAS and APS wrote the paper. All authors critically read the text and
452 approved the manuscript.
453

454 ***Acknowledgements***

455 We would like to acknowledge the funding from Fundação de Amparo à Pesquisa do Estado
456 de São Paulo (FAPESP 2015/09202-0), Coordenação de Aperfeiçoamento de Pessoal de
457 Nível Superior (CAPES, Computational Biology Program) and Conselho Nacional de
458 Desenvolvimento Científico e Tecnológico (CNPq).

459

460 ***Authors' information***

461 [1]Center for Molecular Biology and Genetic Engineering (CBMEG), University of Campinas
462 (UNICAMP), Campinas, SP, Brazil. [2]Graduate Program in Genetics and Molecular Biology,
463 Institute of Biology, UNICAMP, Campinas, SP, Brazil. [3]Holzforshung München, TUM
464 School of Life Sciences Weihenstephan, Technische Universität München, 85354 Freising,
465 Germany. [4]Department of Plant Biology, Institute of Biology, UNICAMP, Campinas, SP,
466 Brazil.

467

468 **References**

469 1. Elad Y, Chet I, Katan J. *Trichoderma harzianum*: a biocontrol agent effective against
470 *Sclerotium rolfsii* and *Rhizoctonia solani*. Phytopathology. 1980;70:119-21.
471 2. Delabona PDS, Farinas CS, da Silva MR, Azzoni SF, Pradella JGC. Use of a new
472 *Trichoderma harzianum* strain isolated from the Amazon rainforest with pretreated

sugar cane bagasse for on-site cellulase production. Bioresour Technol. 2012;107:517-21.

3. Horta MA, Vicentini R, Pda SD, Laborda P, Crucello A, Freitas S, et al. Transcriptome profile of *Trichoderma harzianum* IOC-3844 induced by sugarcane bagasse. PLoS One. 2014;9:e88689.

4. Delabona PDS, Rodrigues GN, Zubieta MP, Ramoni J, Codima CA, Lima DJ, et al. The relation between xyr1 overexpression in *Trichoderma harzianum* and sugarcane bagasse saccharification performance. J Biotechnol. 2017;246:24-32.

5. de Castro AM, Pedro KCNR, da Cruz JC, Ferreira MC, Leite SGF, Pereira N. *Trichoderma harzianum* IOC-4038: a promising strain for the production of a cellulolytic complex with significant β-glucosidase activity from sugarcane bagasse cellulignin. Appl Biochem Biotechnol. 2010;162:2111-22.

6. Santos CA, Zanphorlin LM, Crucello A, Tonoli CC, Ruller R, Horta MA, et al. Crystal structure and biochemical characterization of the recombinant ThBgl, a GH1 β-glucosidase overexpressed in *Trichoderma harzianum* under biomass degradation conditions. Biotechnol Biofuels. 2016;9:71.

7. Filho JAF, Horta MAC, Beloti LL, dos Santos CA, de Souza AP. Carbohydrate-active enzymes in *Trichoderma harzianum*: a bioinformatic analysis bioprospecting for key enzymes for the biofuels industry. BMC Genomics. 2017;18:779.

8. Polikarpov I. Structure and function of enzymes and auxiliary proteins from *Trichoderma*, active in cell-wall hydrolysis/center of biological and industrial process for biofuels - CeProBIO. São Carlos, SP: IFSC/USP; 2017.

9. Lopez-Ramirez N, Volke-Sepulveda T, Gaime-Perraud I, Saucedo-Castañeda G, Favela-Torres E. Effect of stirring on growth and cellulolytic enzymes production by

Trichoderma harzianum in a novel bench-scale solid-state fermentation bioreactor. Bioresour Technol. 2018;265:291-8.

10. Santos CA, Morais MAB, Terrett OM, Lyczakowski JJ, Zanphorlin LM, Ferreira-Filho JA, et al. An engineered GH1 beta-glucosidase displays enhanced glucose tolerance and increased sugar release from lignocellulosic materials. Sci Rep. 2019;9:4903.

11. Bischof RH, Ramoni J, Seiboth B. Cellulases and beyond: the first 70 years of the enzyme producer *Trichoderma reesei*. Microb Cell Fact. 2016;15:106.

12. Martinez D, Berka RM, Henrissat B, Saloheimo M, Arvas M, Baker SE, et al. Genome sequencing and analysis of the biomass-degrading fungus *Trichoderma reesei* (*syn. Hypocrea jecorina*). Nat Biotechnol. 2008;26:553-60.

13. Jun H, Kieselbach T, Jönsson LJ. Enzyme production by filamentous fungi: analysis of the secretome of *Trichoderma reesei* grown on unconventional carbon source. Microb Cell Fact. 2011;10:68.

14. Häkkinen M, Arvas M, Oja M, Aro N, Penttilä M, Saloheimo M, et al. Re-annotation of the CAZy genes of *Trichoderma reesei* and transcription in the presence of lignocellulosic substrates. Microb Cell Fact. 2012;11:134.

15. Alvira P, Gyalai-Korpos M, Barta Z, Oliva JM, Réczey K, Ballesteros M. Production and hydrolytic efficiency of enzymes from *Trichoderma reese* iRUTC30 using steam pretreated wheat straw as carbon source. J Chem Technol Biotechnol. 2013;88:1150-6.

16. Li Y-H, Zhang X-Y, Zhang F, Peng L-C, Zhang D-B, Kondo A, et al. Optimization of cellulolytic enzyme components through engineering *Trichoderma reesei* and on-site fermentation using the soluble inducer for cellulosic ethanol production from corn stover. Biotechnol Biofuels. 2018;11:49.

17. Bischof R, Fourtis L, Limbeck A, Gamauf C, Seiboth B, Kubicek CP. Comparative analysis of the *Trichoderma reesei* transcriptome during growth on the cellulase inducing substrates wheat straw and lactose. Biotechnol Biofuels. 2013;6:127.

18. Gupta VK, Steindorff AS, de Paula RG, Silva-Rocha R, Mach-Aigner AR, Mach RL, et al. The post-genomic era of *Trichoderma reesei*: what's next? Trends Biotechnol. 2016;34:970-82.

19. Santos CA, Ferreira-Filho JA, O'Donovan A, Gupta VK, Tuohy MG, Souza AP. Production of a recombinant swollenin from *Trichoderma harzianum* in *Escherichia coli* and its potential synergistic role in biomass degradation. Microb Cell Fact. 2017;16:83.

20. Villares A, Moreau C, Bennati-Granier C, Garajova S, Foucat L, Falourd X, et al. Lytic polysaccharide monooxygenases disrupt the cellulose fibers structure. Sci Rep. 2017;7:40262.

21. Benocci T, Aguilar-Pontes MV, Zhou M, Seiboth B, de Vries RP. Regulators of plant biomass degradation in *Ascomycetous fungi*. Biotechnol Biofuels. 2017;10:152.

22. Coradetti ST, Craig JP, Xiong Y, Shock T, Tian C, Glass NL. Conserved and essential transcription factors for cellulase gene expression in ascomycete *Fungi*. Proc Natl Acad Sci U S A. 2012;109:7397-402.

23. Liu F, Xue Y, Liu J, Gan L, Long M. ACE3 as a master transcriptional factor regulates cellulase and xylanase production in *Trichoderma orientalis* EU7-22. BioResources. 2018;13:6790-801.

24. Crucello A, Sforça DA, Horta MAC, dos Santos CA, Viana AJC, Beloti LL, et al. Analysis of genomic regions of *Trichoderma harzianum* IOC-3844 related to biomass degradation. PLoS One. 2015;10:e0122122.

546 25. Himmel ME, Ding S-Y, Johnson DK, Adney WS, Nimlos MR, Brady JW, et al.
547 Biomass recalcitrance: engineering plants and enzymes for biofuels production.
548 Science. 2007;315:804-7.
549 26. van den Brink J, de Vries RP. Fungal enzyme sets for plant polysaccharide
550 degradation. Appl Microbiol Biotechnol. 2011;91:1477-92.
551 27. Van Dyk JS, Pletschke BI. A review of lignocellulose bioconversion using enzymatic
552 hydrolysis and synergistic cooperation between enzymes—Factors affecting enzymes,
553 conversion and synergy. Biotechnol Adv. 2012;30:1458-80.
554 28. Nitta M, Furukawa T, Shida Y, Mori K, Kuhara S, Morikawa Y, et al. A new Zn (II)
555 2Cys6-type transcription factor BglR regulates β-glucosidase expression in
556 *Trichoderma reesei*. Fungal Genet Biol. 2012;49:388-97.
557 29. Häkkinen M, Valkonen MJ, Westerholm-Parvinen A, Aro N, Arvas M, Vitikainen M,
558 et al. Screening of candidate regulators for cellulase and hemicellulase production in
559 *Trichoderma reesei* and identification of a factor essential for cellulase production.
560 Biotechnol Biofuels. 2014;7:14.
561 30. Westereng B, Loose JS, Vaaje-Kolstad G, Aachmann FL, Sørlie M, Eijsink VG.
562 Analytical tools for characterizing cellulose-active lytic polysaccharide
563 monooxygenases (LPMOs). Methods Mol Biol. 2018;1796:219-46.
564 31. Toyotome T, Hamada S, Yamaguchi S, Takahashi H, Kondoh D, Takino M, et al.
565 Comparative genome analysis of *Aspergillus flavus* clinically isolated in Japan. DNA
566 Res. 2018;26:95-103.
567 32. Baroncelli R, Piaggeschi G, Fiorini L, Bertolini E, Zapparata A, Pè ME, et al. Draft
568 whole-genome sequence of the biocontrol agent *Trichoderma harzianum* T6776.
569 Genome Announc. 2015;3:e00647-15.

570 33. Kubicek CP, Steindorff AS, Chenthamara K, Manganiello G, Henrissat B, Zhang J, et
571 al. Evolution and comparative genomics of the most common *Trichoderma* species.
572 BMC Genomics. 2019;20:485.
573 34. Li W-C, Huang C-H, Chen C-L, Chuang Y-C, Tung S-Y, Wang T-F. *Trichoderma*
574 *reesei* complete genome sequence, repeat-induced point mutation, and partitioning of
575 CAZyme gene clusters. Biotechnol Biofuels. 2017;10:170.
576 35. Horta MAC, Filho JAF, Murad NF, Santos EO, dos Santos CA, Mendes JS, et al.
577 Network of proteins, enzymes and genes linked to biomass degradation shared by
578 *Trichoderma* species. Sci Rep. 2018;8:1341.
579 36. Kuan CS, Yew SM, Toh YF, Chan CL, Ngeow YF, Lee KW, et al. Dissecting the
580 fungal biology of *Bipolaris papendorfii*: from phylogenetic to comparative genomic
581 analysis. DNA Res. 2015;22:219-32.
582 37. Haitjema CH, Gilmore SP, Henske JK, Solomon KV, de Groot R, Kuo A, et al. A
583 parts list for fungal cellulosomes revealed by comparative genomics. Nat Microbiol.
584 2017;2:17087.
585 38. Wang R, Dong L, He R, Wang Q, Chen Y, Qu L, et al. Comparative genomic
586 analyses reveal the features for adaptation to nematodes in *Fungi*. DNA Res.
587 2018;25:245-56.
588 39. Xie B-B, Qin Q-L, Shi M, Chen L-L, Shu Y-L, Luo Y, et al. Comparative genomics
589 provide insights into evolution of *Trichoderma* nutrition style. Genome Biol Evol.
590 2014;6:379-90.
591 40. Hassan L, Lin L, Sorek H, Sperl LE, Goudoulas T, Hagn F, et al. Crosstalk of
592 cellulose and mannan perception pathways leads to inhibition of cellulase production
593 in several *Filamentous fungi*. MBio. 2019;10:e00277-19.

41. Ivanova C, Ramoni J, Aouam T, Frischmann A, Seiboth B, Baker SE, et al. Genome sequencing and transcriptome analysis of *Trichoderma reesei* QM9978 strain reveals a distal chromosome translocation to be responsible for loss of vib1 expression and loss of cellulase induction. Biotechnol Biofuels. 2017;10:209.

42. Lawler K, Hammond-Kosack K, Brazma A, Coulson RM. Genomic clustering and co-regulation of transcriptional networks in the pathogenic fungus *Fusarium graminearum*. BMC Syst Biol. 2013;7:52.

43. Castro LDS, Pedersoli WR, Antoniêto ACC, Steindorff AS, Silva-Rocha R, Martinez-Rossi NM, et al. Comparative metabolism of cellulose, sophorose and glucose in Trichoderma reesei using high-throughput genomic and proteomic analyses. Biotechnol Biofuels. 2014;7:41.

44. Berlin K, Koren S, Chin C-S, Drake JP, Landolin JM, Phillippy AM. Assembling large genomes with single-molecule sequencing and locality-sensitive hashing. Nat Biotechnol. 2015;33:623-30.

45. Myers EW, Sutton GG, Delcher AL, Dew IM, Fasulo DP, Flanigan MJ, et al. A whole-genome assembly of *Drosophila*. Science. 2000;287:2196-204.

46. Chaisson MJ, Tesler G. Mapping single molecule sequencing reads using basic local alignment with successive refinement (BLASR): application and theory. BMC Bioinformatics. 2012;13:238.

47. Chin C-S, Alexander DH, Marks P, Klammer AA, Drake J, Heiner C, et al. Nonhybrid, finished microbial genome assemblies from long-read SMRT sequencing data. Nat Methods. 2013;10:563-9.

48. Salamov AA, Solovyev VV. Ab initio gene finding in *Drosophila* genomic DNA. Genome Res. 2000;10:516-22.

618 49. Conesa A, Götz S, García-Gómez JM, Terol J, Talón M, Robles M. Blast2GO: a
619 universal tool for annotation, visualization and analysis in functional genomics
620 research. Bioinformatics. 2005;21:3674-6.
621 50. Mitchell A, Chang H-Y, Daugherty L, Fraser M, Hunter S, Lopez R, et al. The
622 InterPro protein families database: the classification resource after 15 years. Nucleic
623 Acids Res. 2015;43:D213-21.
624 51. Kurtz S, Phillippy A, Delcher AL, Smoot M, Shumway M, Antonescu C, et al.
625 Versatile and open software for comparing large genomes. Genome Biol. 2004;5:R12.
626 52. Veltri D, Wight MM, Crouch JA. Simple synteny: a web-based tool for visualization
627 of microsynteny across multiple species. Nucleic Acids Res. 2016;44:W41-5.
628 53. Thompson JD, Higgins DG, Gibson TJ. CLUSTAL W: improving the sensitivity of
629 progressive multiple sequence alignment through sequence weighting, position-
630 specific gap penalties and weight matrix choice. Nucleic Acids Res. 1994;22:4673-80.
631 54. Kumar S, Stecher G, Tamura K. MEGA7: molecular evolutionary genetics analysis
632 version 7.0 for bigger datasets. Mol Biol Evol. 2016;33:1870-4.
633 55. Jones DT, Taylor WR, Thornton JM. The rapid generation of mutation data matrices
634 from protein sequences. Comput Appl Biosci. 1992;8:275-82.
635 56. Felsenstein J. Confidence limits on phylogenies: an approach using the bootstrap.
636 Evolution. 1985;39:783-91.
637 57. Källberg M, Margaryan G, Wang S, Ma J, Xu J. RaptorX server: a resource for
638 template-based protein structure modeling. In: Kihara D, editor. Protein structure
639 prediction. New York, NY: Springer; 2014. p. 17-27.
640 58. CLC Genomics Workbench 9.0. Qiagen (Aarhus A/S). Manual for CLC genomics
641 workbench 9.0 windows, Mac OS X and Linux Denmark. 2016.

59. Wilczynski B, Dojer N. BNFinder: exact and efficient method for learning bayesian networks. Bioinformatics. 2009;25:286-7.

60. Shannon P, Markiel A, Ozier O, Baliga NS, Wang JT, Ramage D, et al. Cytoscape: a software environment for integrated models of biomolecular interaction networks. Genome Res. 2003;13:2498-504.

667 **Figure legends**

668 **Figure 1.** Distribution of the *T. harzianum* IOC3844 genes on the 1 Mb intervals of the seven
669 chromosomes of *T. reesei* QM6a. CAZyme genes of *T. harzianum* IOC3844 are in red,
670 CAZymes genes of *T. reesei* are in blue, and all genes of *T. harzianum* IOC3844 are in green.
671 Th: *T. harzianum* IOC3844; Tr: *T. reesei* QM6a.

672 **Figure 2.** Functional annotation of the genes predicted in the genomic regions of *T.*
673 *harzianum* IOC3844. Annotation of genes for gene ontologies for biological processes,
674 cellular components and molecular functions. (a) Distribution of enzymes annotated
675 according to enzyme commission (b) and major enzyme commission (EC) related to cellulose
676 and hemicellulose degradation (c).

677 **Figure 3.** CAZy classification of genes annotated in the genomic regions of *T. harzianum*
678 IOC3844. GH: glycoside hydrolases; GT: glycosyl transferases; PLs: polysaccharide lyases;
679 CEs: carbohydrate esterases; AA: auxiliary activities; CBM: carbohydrate-binding modules.

680 **Figure 4.** Comparison between the gene clusters of *T. harzianum* IOC3844 and those of other
681 species of the genus *Trichoderma* spp. GH1: glycoside hydrolase 1; GH4: glycoside
682 hydrolase 4; MFS: major facilitator superfamily permease; Trans: putative transporter; TF-1:
683 putative transcription factor 1; GT38: glycosyl transferases 4; CBM18: carbohydrate-binding
684 modules 18; TF-2: putative transcription factor 2; CLR2: cellulose regulator 2; GH2:
685 glycoside hydrolase 2; GH26: glycoside hydrolase 26; Th: *T. harzianum*; Tv: *T. virens*; Ta: *T.*
686 *atroviride*; Tr: *T. virens*.

687 **Figure 5.** Molecular phylogeny of the CLR2 transcription factor in Ascomycota and
688 Basidiomycota (a); *in silico* protein modeling for CLR2 in *T. harzianum* IOC3844 (b) and *T.*
689 *reesei* QM6a (c).

Figure 6. Subnetwork of CLR2 transcription factors and related genes (a) and network of induced (blue) and repressed (red) genes under cellulose conditions (b). CLR2: cellulose regulator 2; GH: glycoside hydrolases; GT: glycosyl transferases; AA: auxiliary activities.

Figure 7. Molecular scheme of the enzymatic model in the degradation of cellulose in *Trichoderma* spp. Enzymes and PDB code: beta-glucosidase (5BWF), cellobiohydrolase I (2YOK), cellobiohydrolase II (1CB2), endoglucanase 3 (4H7M), copper-dependent lytic polysaccharide mono-oxygenases (LPMOs) (5O2W).

719 **Table 1.** Proteins identified in genomic and in the *T. harzianum* IOC3844 secretome under
720 cellulose growth conditions.

IDs*	Protein name	Secretome/UniProt ID	CAZy family	CEL (TPM)	GLI (TPM)
1010	Hypothetical protein	A0A0G0ALT6	GH28	14.2	6.2
1043	Cellulosome enzyme	A0A0G0A296	GH30	35.6	11.5
1054	Glycosyl hydrolase 10	A0A0F9X8A4	GH10	14.8	4.1
1075	Glycosyl hydrolase 64	A0A0F9ZIR5	GH64	824.3	262.4
1095	Glycosyl hydrolase 18	A0A0F9ZHI0	GH18	83.2	47.9
11	Mutanase	A0A0F9XN06	CBM24	2741.6	1452.9
1133	Glycosyl hydrolase 12	A0A0F9Y2E9	GH12	1579.8	308.2
1150	Glycosyl hydrolase 47	A0A0F9WYR7	GH47	83.9	74.6
1217	Beta-mannosidase	A0A0F9ZDV4	GH2	117.9	124.2
126	Glycosyl hydrolase 76	A0A0F9X1Q3	GH76	616.7	375.4
1318	Beta-xylosidase	A0A0G0A408	GH3	172.3	125.2
1439	Alpha-L-arabinofuranosidase B	A0A0G0A4Q2	CBM42	450.4	343.5
1440	Glycosyl hydrolase 3	A0A0F9XRC5	GH3	245.8	107.4
1498	WSC domain-containing	A0A0F9ZXC9	AA5_1	342.5	339.0
44	Beta-1,3-	A0A0F9ZKA8	GH72	2431.7	3210.5

	glucanosyltransferase				
441	Alpha-glucosidase	A0A0G0AG54	GH31	2121.6	1655.2
559	Alpha-1,2-mannosidase	A0A0G0ABI9	GH92	226.9	153.4
666	Glycosyl hydrolase 3	A0A0F9XQT4	GH3	77.2	43.0
667	Hypothetical protein	A0A0G0AME2	CBM1	874.9	142.8
668	Glycosyl hydrolase 61	A0A0F9XMI8	AA9	3109.7	625.1
669	Glycosyl hydrolase 16	A0A0F9XP75	CBM13	16.4	3.7
671	Cytochrome P450 monooxygenase	A0A0G0A4Z5	GT4	1569.5	1595.3
681	Glycosyl hydrolase 11	A0A0F9Y0Y9	GH11/CBM1	4206.8	1316.1
741	Endo-N-acetyl-beta-D-glucosaminidase	A0A0F9ZHA7	GH18	3971.9	2328.0
759	Hypothetical protein	A0A0F9ZJ74	GH20	1184.8	1507.7
813	Catalase peroxidase	A0A0F9X3Z8	AA2	2677.7	2473.4
82	Glycosyl hydrolase 6	A0A0G0AEM7	GH6/CBM1	5843.5	1567.4
842	Hypothetical protein	A0A0F9XY55	GH45/CBM1	41.3	15.3
9	Glycosyl hydrolase 62	A0A0F9X8Z0	GH62	353.9	103.4
913	Isoamyl alcohol oxidase	A0A0F9XC99	AA7	39.3	13.2
918	Hypothetical protein	A0A0F9XG06	GH5_5	870.8	750.9

721 *****The annotated genes IDs can be found in Supplementary Table S4

722

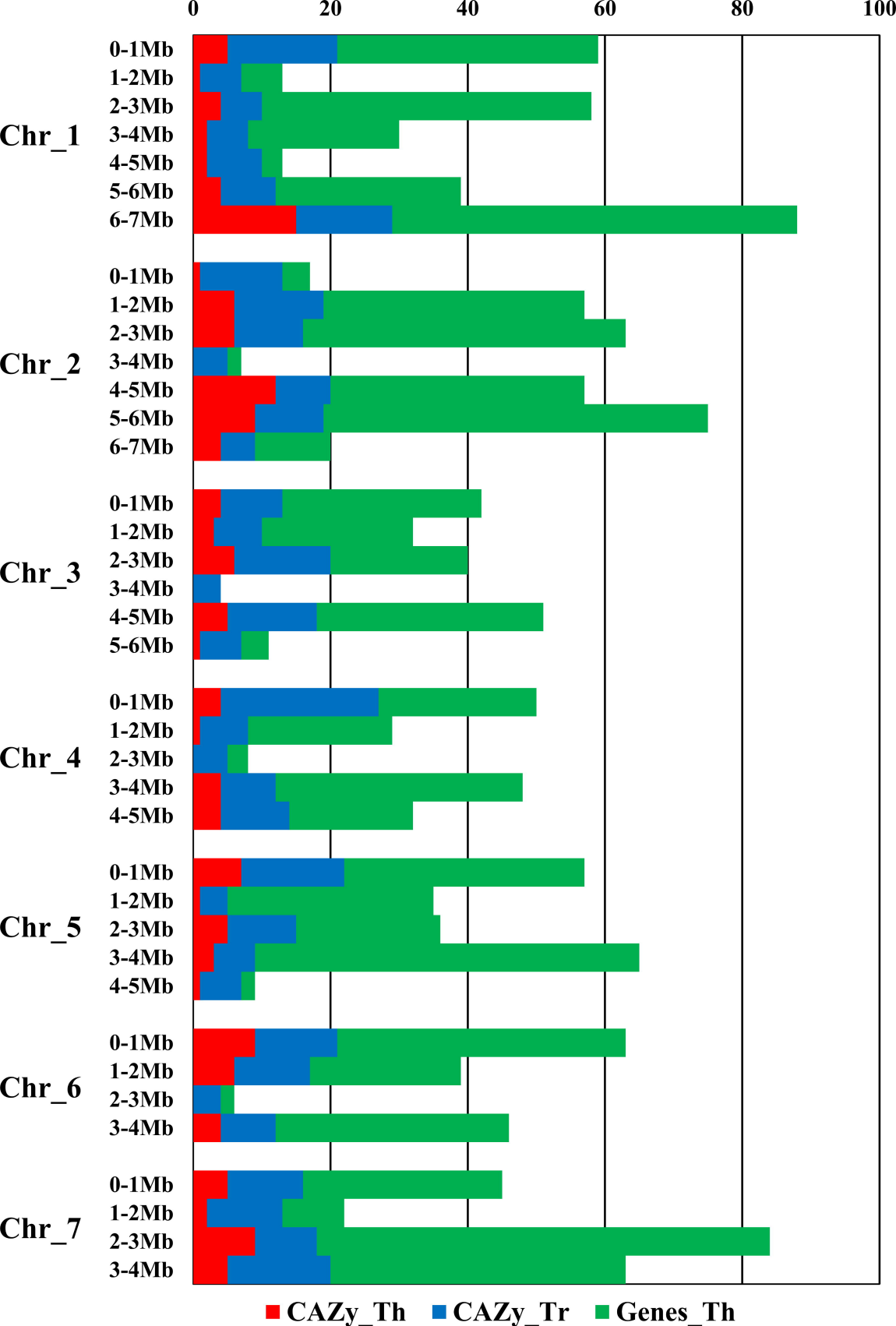
0
20
40
60
80
100
Chr_1
0-1Mb
1-2Mb
2-3Mb
3-4Mb
4-5Mb
5-6Mb
6-7Mb
Chr_2
0-1Mb
1-2Mb
2-3Mb
3-4Mb
4-5Mb
5-6Mb
6-7Mb
Chr_3
0-1Mb
1-2Mb
2-3Mb
3-4Mb
4-5Mb
5-6Mb
Chr_4
0-1Mb
1-2Mb
2-3Mb
3-4Mb
4-5Mb
Chr_5
0-1Mb
1-2Mb
2-3Mb
3-4Mb
4-5Mb
Chr_6
0-1Mb
1-2Mb
2-3Mb
3-4Mb
Chr_7
0-1Mb
1-2Mb
2-3Mb
3-4Mb
CAZy_Th
CAZy_Tr
Genes_Th

a

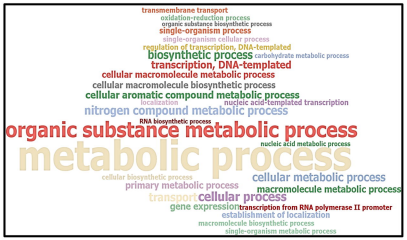
Biological Process
transmembrane transport
oxidation-reduction process
organic substance biosynthetic process
single-organism process
single-organism cellular process
regulation of transcription, DNA-templated
biosynthetic process
carbohydrate metabolic process
transcription, DNA-templated
cellular macromolecule metabolic process
cellular macromolecule biosynthetic process
cellular aromatic compound metabolic process
biosynthetic process
nucleic acid-templated transcription
nitrogen compound metabolic process
RNA biosynthetic process
organic substance metabolic process
nucleic acid metabolic process
metabolic process
cellular biosynthetic process
cellular metabolic process
primary metabolic process
macromolecule metabolic process
transport
cellular process
gene expression
transcription from RNA polymerase II promoter
establishment of localization
macromolecule biosynthetic process
single-organism metabolic process

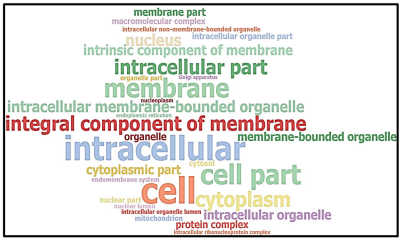
Cellular Component
membrane part
macromolecular complex
intracellular non-membrane-bounded organelle
nucleus
intracellular organelle part
intrinsic component of membrane
intracellular part
organelle part
cell wall
membrane
nucleoplasm
intracellular membrane-bounded organelle
integral component of membrane
organelle
membrane-bounded organelle
intracellular
cytoplasmic part
cytosol
endomembrane system
cell
cell part
nuclear part
endoplasmic reticulum
cytoplasm
nucleolus
intracellular organelle lumen
intracellular organelle
mitochondrion
protein complex
ribonucleoprotein complex

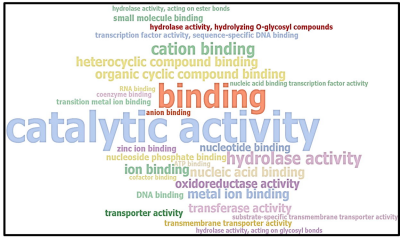
Molecular Function
hydrolase activity, acting on ester bonds
small molecule binding
hydrolase activity, hydrolyzing O-glycosyl compounds
transcription factor activity, sequence-specific DNA binding
cation binding
heterocyclic compound binding
organic cyclic compound binding
nucleic acid binding transcription factor activity
RNA binding
coenzyme binding
transition metal ion binding
binding
anion binding
catalytic activity
zinc ion binding
nucleotide binding
nucleoside phosphate binding
hydrolase activity
ion binding
nucleic acid binding
cofactor binding
oxidoreductase activity
DNA binding
metal ion binding
transferase activity
transporter activity
substrate-specific transmembrane transporter activity
transmembrane transporter activity
hydrolase activity, acting on glycosyl bonds

b

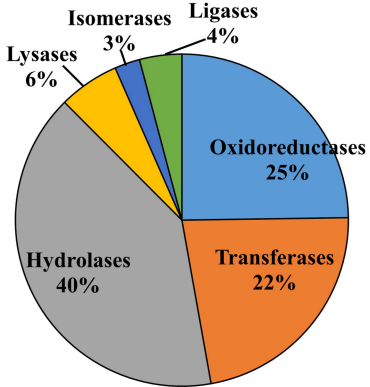
Isomerases
3%
Ligases
4%
Lysases
6%
Oxidoreductases
25%
Hydrolases
40%
Transferases
22%

c

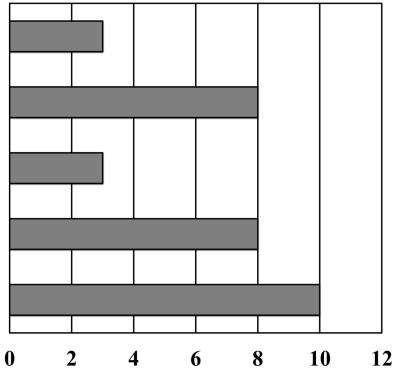
α-L-arabinofurasidase EC 3.2.1.55
endo-1,4-β-xylanase EC 3.2.1.8
cellobiohydrolase EC 3.2.1.91
endo-β-1,4-glucanase EC 3.2.1.4
β-glucosidase EC 3.2.1.21
0
2
4
6
8
10
12

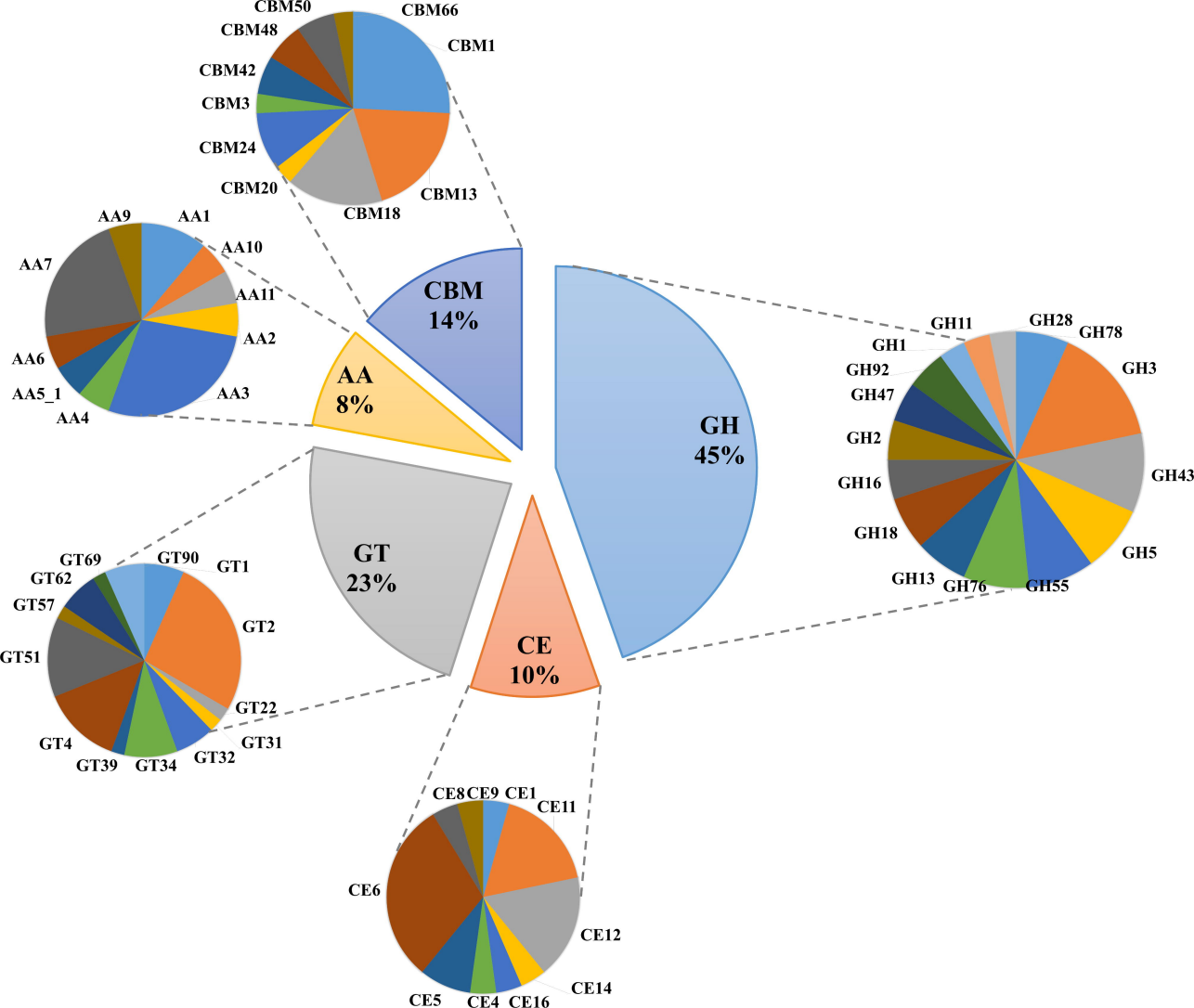
CBM
14%
AA
8%
GT
23%
CE
10%
GH
45%
CBM50
CBM66
CBM48
CBM1
CBM42
CBM3
CBM24
CBM20
CBM13
CBM18
AA9
AA1
AA10
AA7
AA11
AA2
AA6
AA5_1
AA3
AA4
GH11
GH28
GH78
GH1
GH3
GH92
GH47
GH2
GH43
GH16
GH18
GH5
GH13
GH76
GH55
GT69
GT90
GT1
GT62
GT57
GT2
GT51
GT22
GT4
GT31
GT39
GT34
GT32
CE8
CE9
CE1
CE11
CE6
CE12
CE14
CE5
CE4
CE16

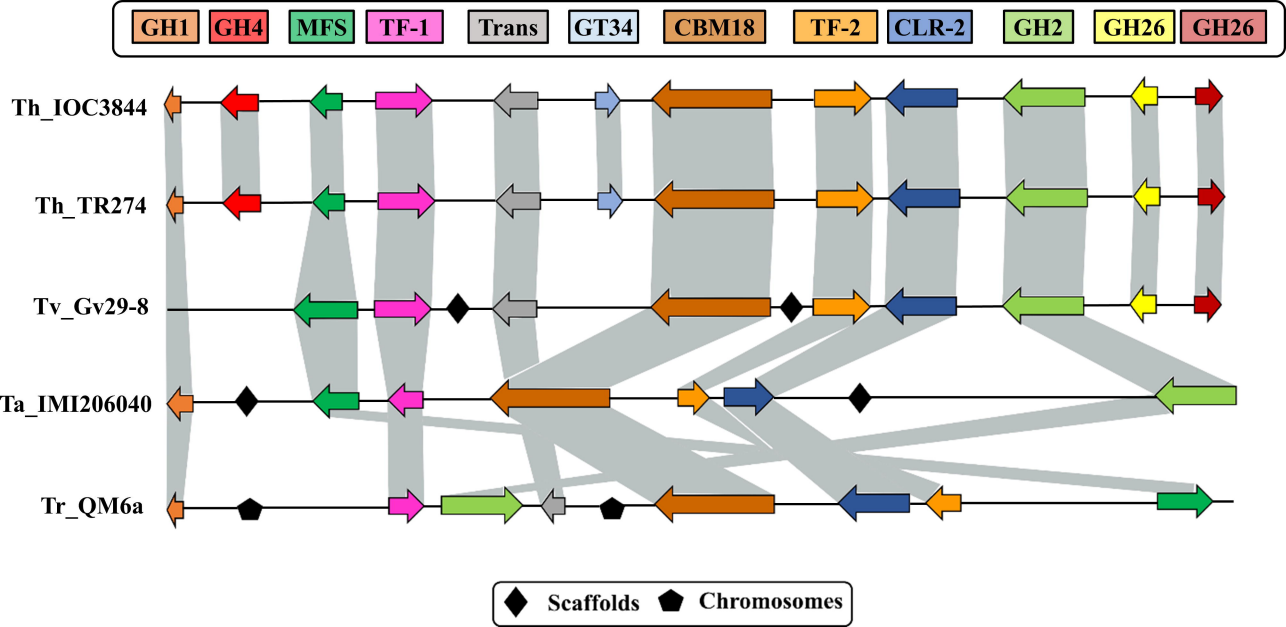
GH1
GH4
MFS
TF-1
Trans
GT34
CBM18
TF-2
CLR-2
GH2
GH26
GH26
Th_IOC3844
Th_TR274
Tv_Gv29-8
Ta_IMI206040
Tr_QM6a
Scaffolds
Chromosomes

Cellulose Degradation Regulator 2 (CLR2)

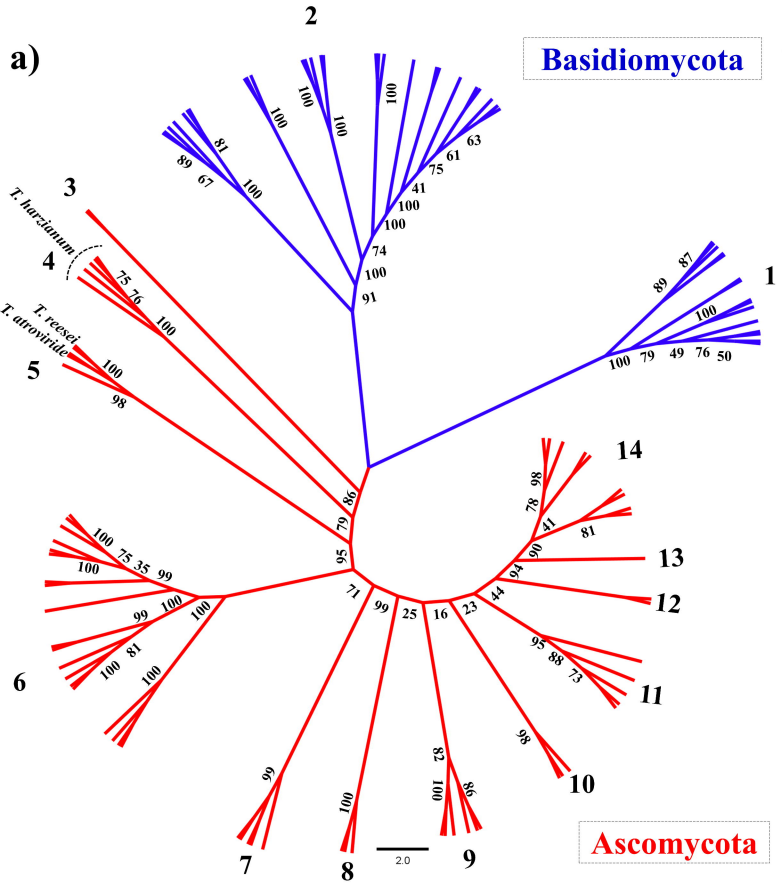

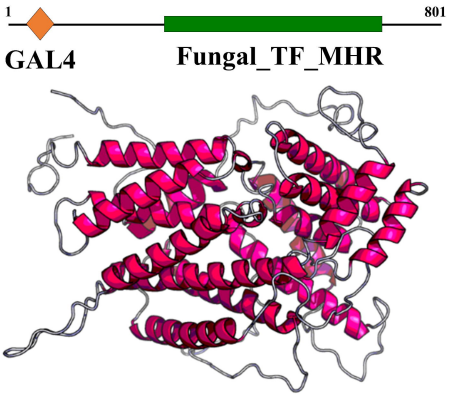

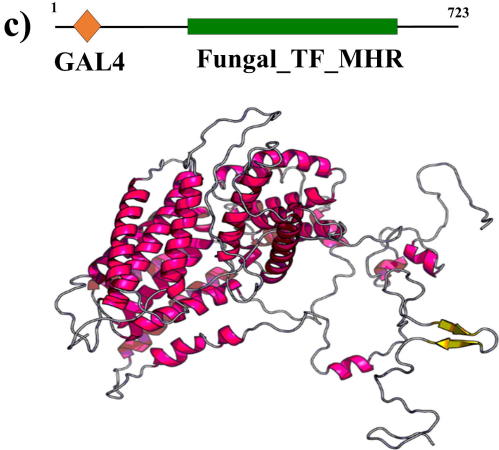

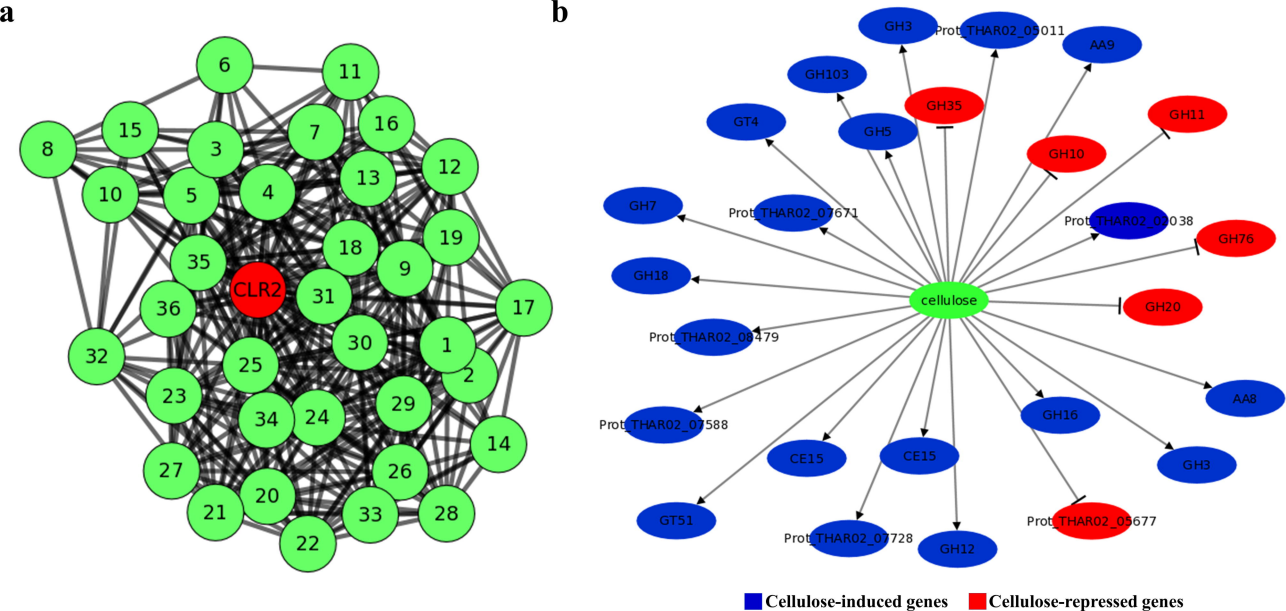
a
6
11
8
15
3
7
16
12
10
5
4
13
18
19
35
CLR2
9
31
17
36
30
1
32
25
2
23
34
24
29
14
27
26
20
21
33
28
22
b
GH3
Prot_THAR02_05011
AA9
GH103
GH35
GH11
GT4
GH5
GH10
GH7
Prot_THAR02_07671
Prot_THAR02_01038
GH76
GH18
cellulose
GH20
Prot_THAR02_06479
AA8
Prot_THAR02_07588
GH16
CE15
CE15
GH3
GT51
Prot_THAR02_05677
Prot_THAR02_07728
GH12
Cellulose-induced genes
Cellulose-repressed genes

Cellulose Degradation

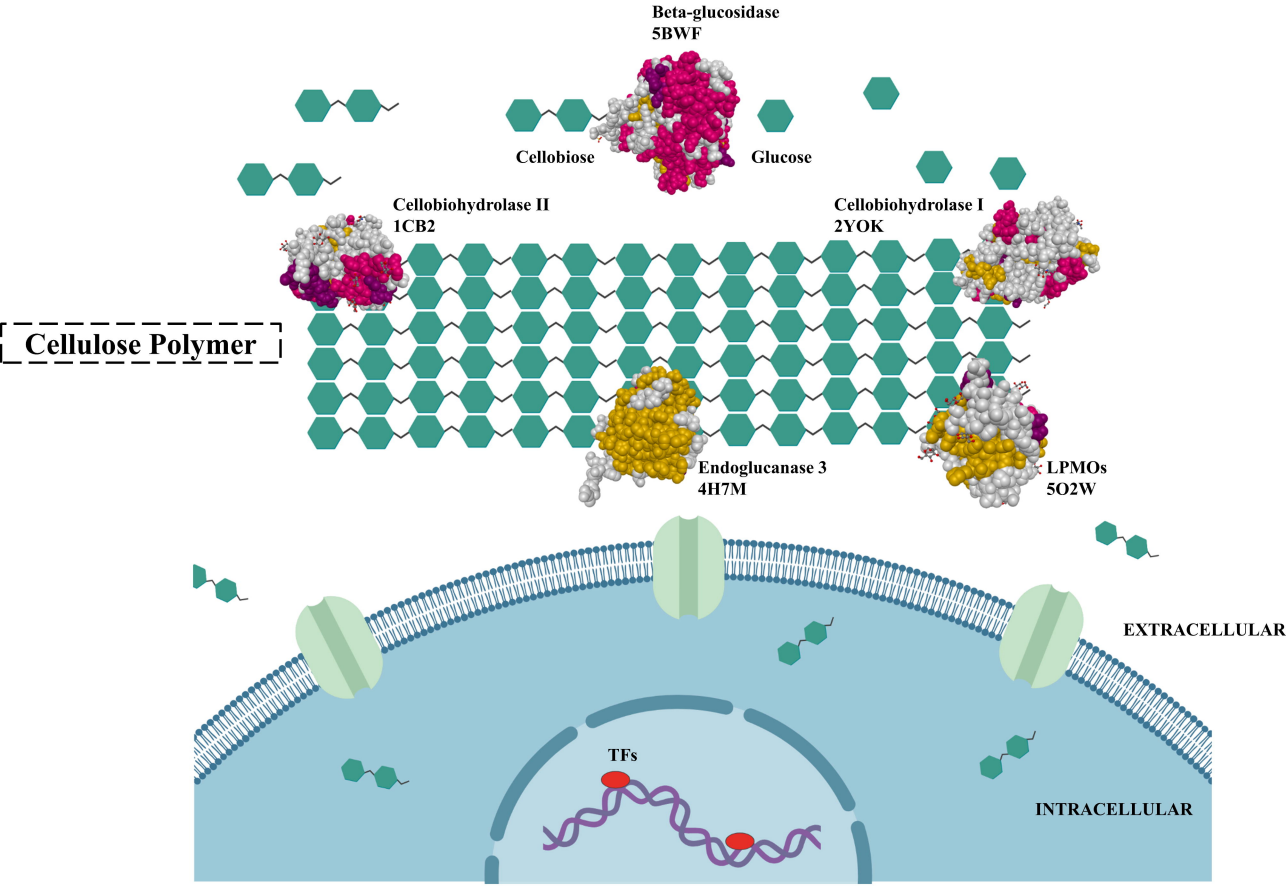

CAZy family	*T. harzianum*	*T. reesei*
GH1	4	2
GH3	17	13
GH6	1	1
GH7	2	2
GH12	3	2
GH45	3	1
AA9	4	3

Ferreira Filho et al., 2017